Herschel M33 Extended Survey
PACS Spectroscopy Along The Major Axis Of M33

Thomas Nikola[1], C. Kramer[2], G.J. Stacey[1], B. Mookerjea[3], F. Israel[4], J. Braine[5], & HerM33es Team
[1] Cornell University, USA, [2] IRAM, Spain, [3] Tata Institute, India, [4] Leiden University, The Netherlands, [5] Université Bordeaux, France

Outline:

The Herschel key program HerM33es (Herschel M33 Extended Survey; PI: Carsten Kramer) aimes to investigate the link between star formation and the galactic environment, including the phases of the interstellar medium (ISM), energy balance of the ISM, and formation of molecular clouds. The nearly face-on and nearby (840 kpc) galaxy M33 is a prime target for this study. As part of this program we have observed a strip along the major axis of M33 in the fine-structure lines [CII] 158 µm, [OI] 63µm, and [NII] 122 µm using PACS on Herschel.

The beam size of our observations is about 12", corresponding to 49 pc at the distance of M33, and is well matched the size of a Giant Molecular Cloud.

We compare our spectral maps with observations of M33 in HI and CO(2-1) (Gratier et al. 2010), Hα (Hoopes & Walterbos 2000), and Spitzer/MIPS 24 µm (Tabatabaei et al. 2007).

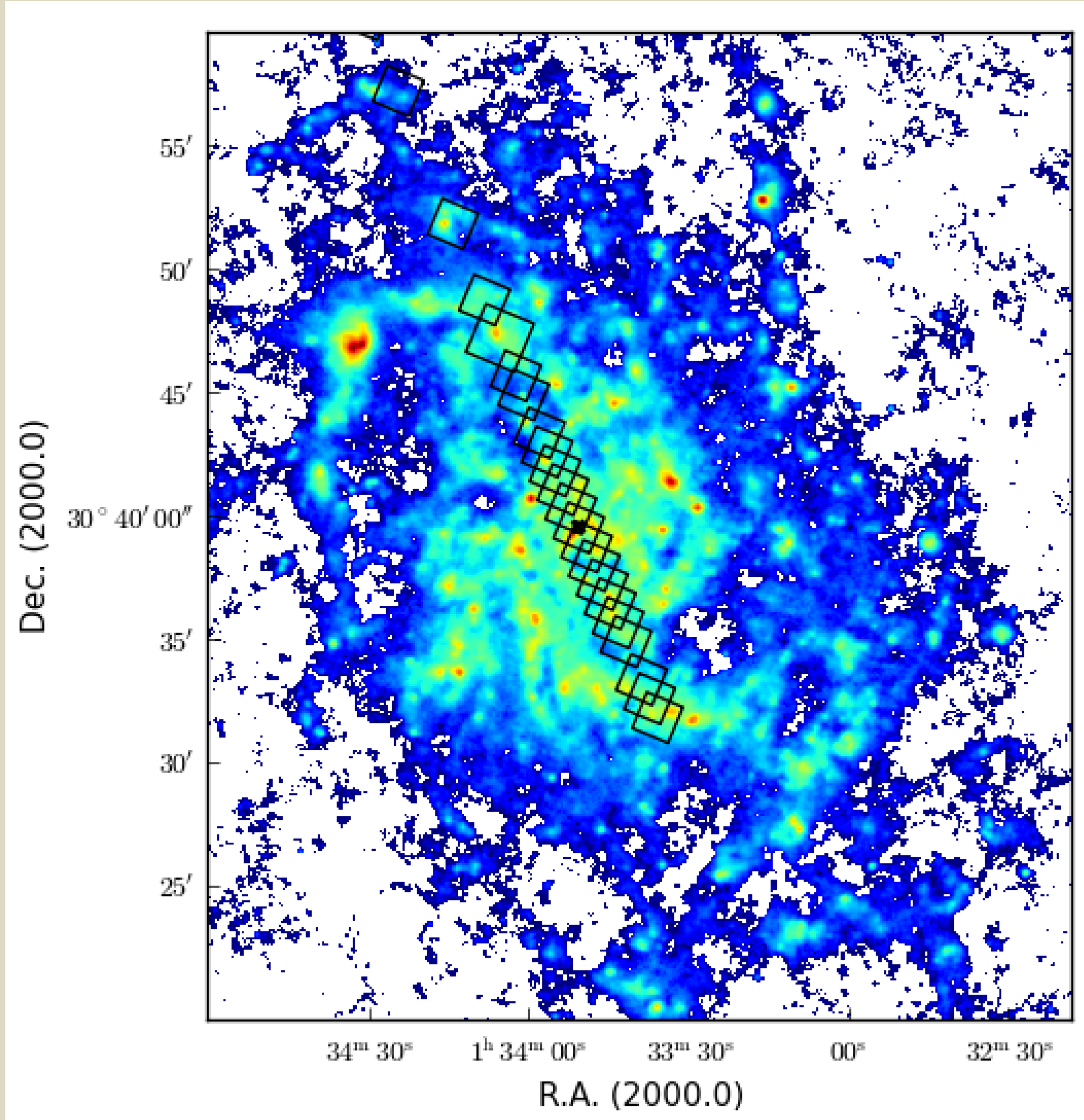

Figure 1: FIR map overplotted with the squares showing the covered regions observed with PACS.

Observation and Data Reduction:

We have observed 22 positions along the major axis of M33 in the [CII] 158 µm, [OI] 63µm, and [NII] 122 µm using PACS (Poglitsch et al. 2010) on Herschel (Pilbratt et al. 2010) in unchopped mode. At each position we obtained fully sampled 95"×95" regions by stepping the detector field of view in a 3×3 raster. The integration time per position was about 7000 sec. The beam sizes are about 9.5", 10", and 11.5" for the [OI], [NII], and [CII] line, and the spectral resolutions are about 90 km/s, 290 km/s, and 240 km/s, respectively (PACS Observer's Manual V2.3).

Dario Fadda (IPAC) provided a script, modifying HIPE ver.7, that allowed to combine the individual observations to a single map.

The line intensities were determined by fitting and subtracting baselines to the spectra and integrating over a velocity range appropriate for the velocity shifts in M33. All maps were smoothed to 12" and reprojected on the [CII] map.

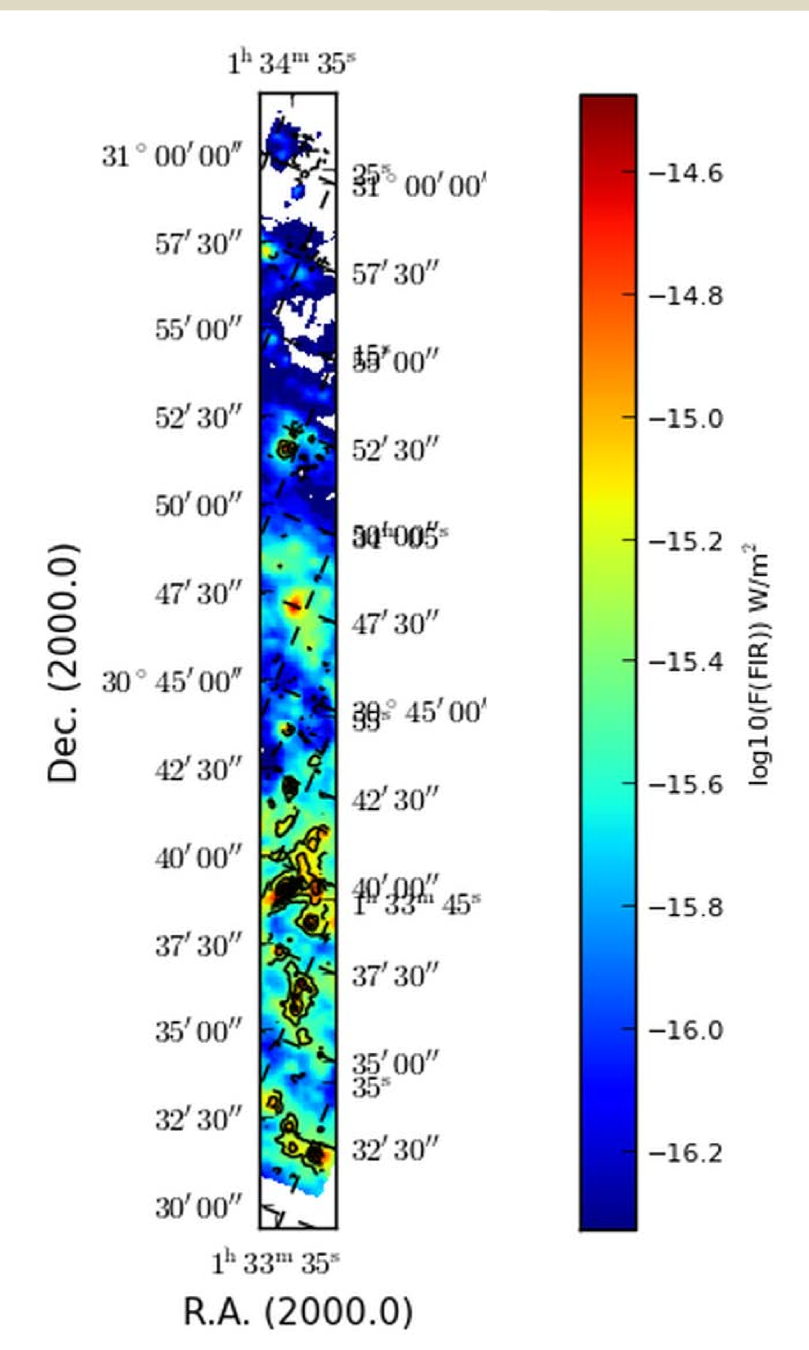

Figure 2: FIR color map along the entire PACS strip overplotted with [CII] contours.

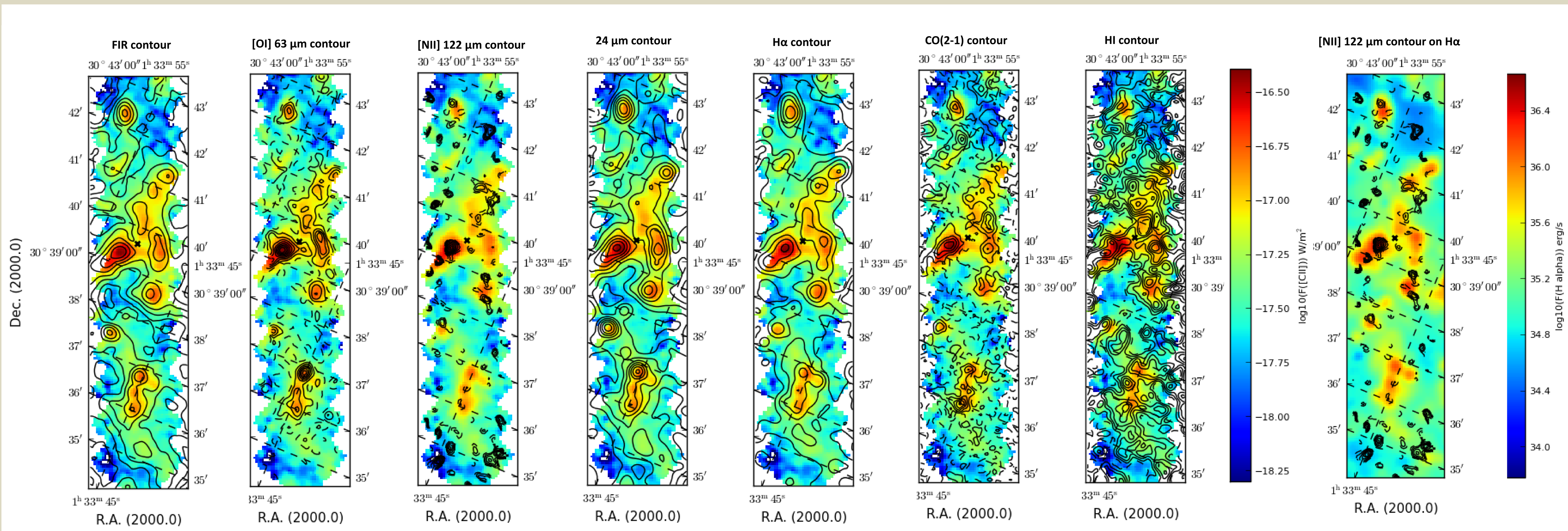

Figure 3: Eight maps of the central region of M33. The seven left most plots show the color map of the [CII] emission in a logarithmic scale overlaid with contour maps of line and continuum tracers for atomic gas ([OI], HI), molecular gas (CO(2-1)), ionized gas (Hα, [NII]), and dust (24µm, FIR).

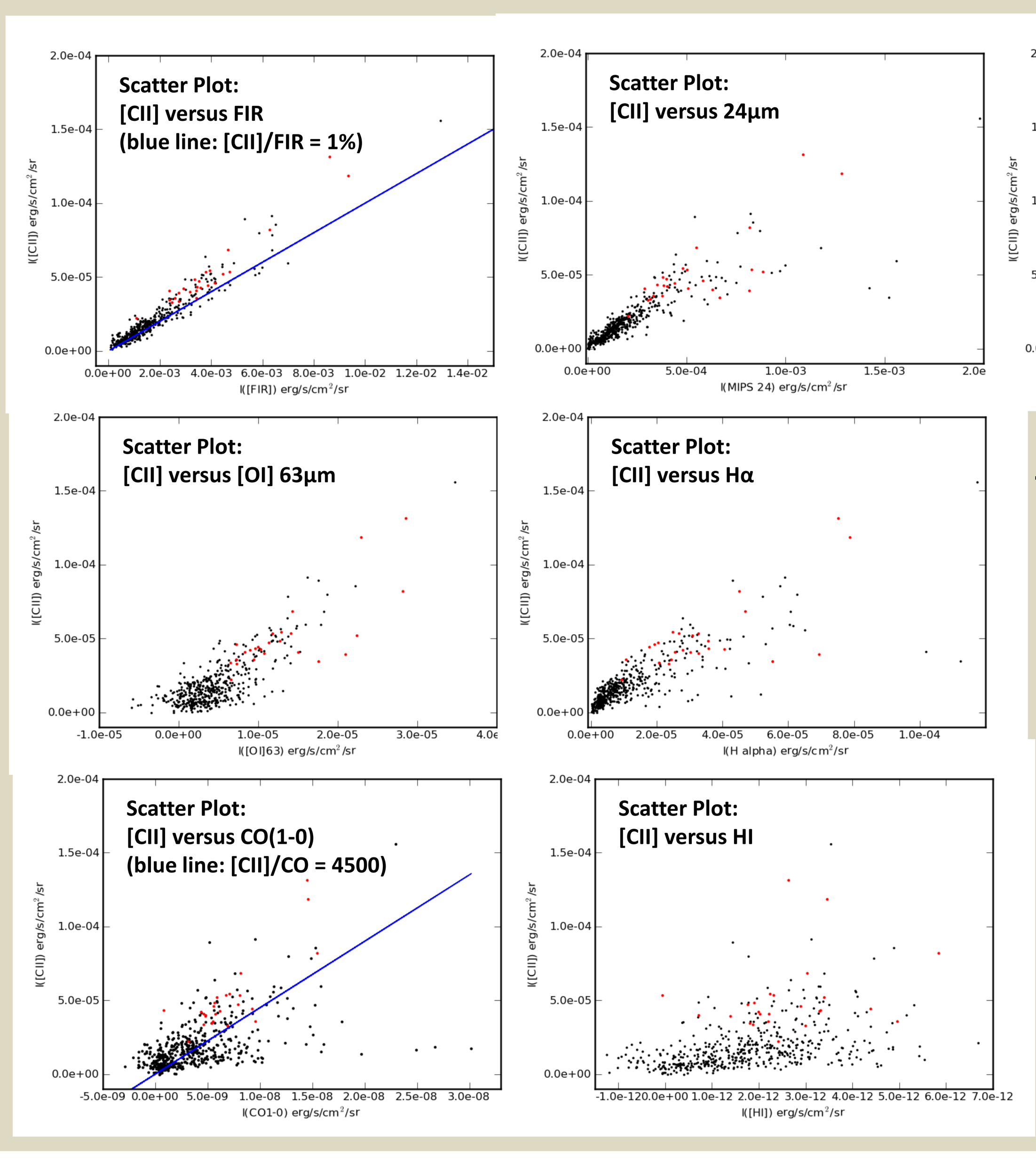

Figure 4: Scatter plot of [CII] and other intensities along the radial PACS strip. The black dots are the intensities of resampled map (5x5 spaxels) and the red dots are the intensities at the [CII] emission peak positions.

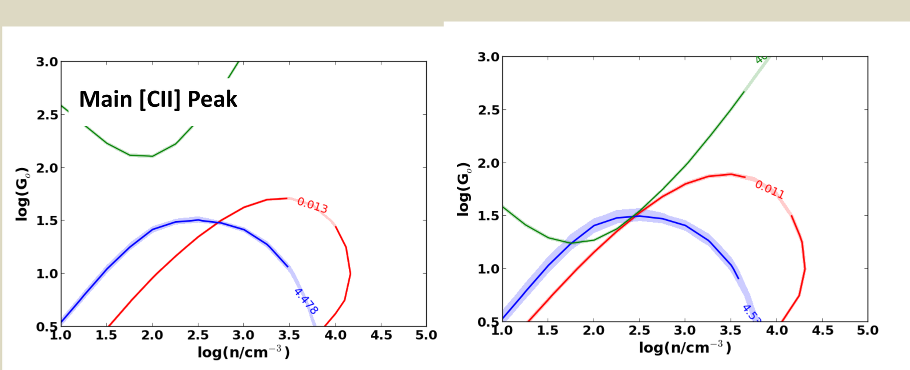

Figure 5: PDR plot of FUV versus hydrogen density for two [CII] peak locations. The contour lines show the range of FUV-n(H) combinations for a specific intensity ratio as predicted by the Kaufman et al. (1999) PDR model. Red contour: [CII]/FIR; blue contour: [CII]/[OI]63; green contour: [CII]/CO(1-0). The shaded regions represents the 1σ uncertainty.

Discussion:

Figure 2 shows that the morphology of the [CII] emission matches very well with the FIR emission along the entire major axis of M33. In Figure 3 we zoom into the central region of M33 and compare the morphology of several line and continuum emissions. The close resemblance between the [CII], [OI], FIR, 24 µm, and Hα indicates that they trace star forming regions in M33. While the CO(2-1) emission is similar in general it exhibits some significant differences. The HI emission is very clumpy and HI peaks do not necessarily coincide with [CII] peaks. The [NII] emission is detected at low signal-to-noise. At strong [CII] peaks we also find [NII] peaks but overall the morphology is different. That is also true for comparison of [NII] with Hα. The scatter plots (Fig. 4) also support the notion that [CII] and [OI] trace star forming region. The scatter plots show that the CO line is strikingly weak compared to the [CII] line. That is also apparent in the PDR (Photodissociation Region) plots in Figure 5, which shows two examples for line ratios found in [CII] peak emission regions.. The [CII]/CO ratio is significantly offset from any PDR solution for many regions. A possible explanation for this finding are CO dark clouds.

References:
Boquien, M., Calzetti, D., Combes, F., et al. 2011, AJ, 142, 111
Gratier, P., Braine, J., Rodriguez-Fernandez, N.J., et al. 2010, A&A, 522, A3
Hoopes, C.G., & Walterbos, R.A.M. 2000, ApJ, 541, 597
Kaufman, M. J., Wolfire, M. G., Hollenbach, D. J., & Luhman, M. L. 1999, ApJ, 527, 795
Kramer, C., Buchbender, C., Xilouris, E.M., et al. 2010, A&A, 518L, 67
Mookerjea, B., Kramer, C., Buchbender, C., et al. 2011, A&A, 532, A152
Pilbratt, G.L., Riedinger, J.R., Passvogel, T., et al. 2010, A&A, 518, L1
Poglitsch, A., Waelkens, C., Geis, N., et al. 2010, A&A, 518, L2
Tabatabaei, F.S., Beck, R., Krause, M., et al. 2007, A&A, 466, 509